SPhT-T04/117

A refined Razumov-Stroganov conjecture II

P. Di Francesco,

Service de Physique Théorique de Saclay,
CEA/DSM/SPhT, URA 2306 du CNRS,
F-91191 Gif sur Yvette Cedex, France

We extend a previous conjecture [1] relating the Perron-Frobenius eigenvector of the monodromy matrix of the O(1) loop model to refined numbers of alternating sign matrices. By considering the O(1) loop model on a semi-infinite cylinder with dislocations, we obtain the generating function for alternating sign matrices with prescribed positions of 1's on their top and bottom rows. This seems to indicate a deep correspondence between observables in both models.

AMS Subject Classification (2000): Primary 05A19; Secondary 82B20

09/2004

1. Introduction: ASM, FPL and the RS conjecture

Alternating sign matrices (ASM), a classical subject of combinatorics, have received lots of attention recently in the more physical context of the fully-packed loop (FPL) model, as well as in relation to the O(1) loop model, via the celebrated Razumov-Stroganov (RS) conjecture.

Alternating sign matrices (ASM) are matrices with entries $0, \pm 1$, such that $+1$'s and -1's alternate along each row and column, possibly separated by arbitrarily many 0's, and such that the entries in each row and column sum to $+1$. The total number of $n \times n$ ASM reads (see [2] for a nice historical exposition of this formula and many references)

$$A_n = \prod_{j=0}^{n-1} \frac{(3j+1)!}{(n+j)!} \tag{1.1}$$

The ASM may be viewed as configurations of the fully-packed loop (FPL) model, in which each of the edges of a square grid of size $n \times n$ of square lattice may be occupied by a bond, in such a way that exactly two bonds are incident to each vertex, and with the boundary condition that every other external edge perpendicular to the boundary of the grid is occupied by a bond. This gives rise to six possible vertex configurations, two of which are "crossing" (bonds occupy opposite edges) and four of which are "turning" (bonds occupy consecutive edges). The 0's of the ASM correspond to turning vertices of the FPL, while ± 1's correspond to crossing vertices.

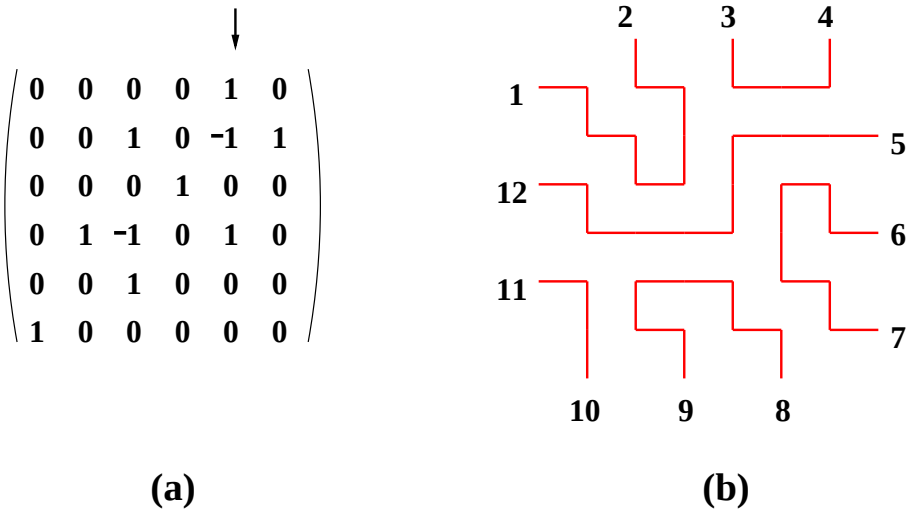

Fig. 1: Two kinds of observables in the ASM/FPL contexts. An ASM (a) of size 6×6 with a 1 in position 5 in its top row (indicated by an arrow). The corresponding FPL configuration (b), with external occupied edges labeled from 1 to 12, has the link pattern (21)(43)(76)(98)(11 10)(12 5).

A natural observable in the context of ASM is the position of the only 1 present in the first row of every such matrix (see Fig.1 (a) for an illustration). The total number $A_{n,m}$ of ASM of size $n \times n$ with a 1 in position m (counted from left) in their top row was conjectured and then proved to read

$$A_{n,m} = \binom{n+m-2}{m-1} \frac{(2n-m-1)!}{(n-m)!} \prod_{j=0}^{n-2} \frac{(3j+1)!}{(n+j)!} \tag{1.2}$$

Another natural observable in the context of FPL is the connectivity of external bonds (see Fig.1 (b) for an illustration). Indeed, the external bonds are connected by pairs via non-intersecting chains of consecutive bonds across the grid. After labeling the external bonds $1, 2, ..., 2n$ clockwise around the grid, these "planar" pairings are recorded by link patterns π, conveniently written as the succession of pairs of connected labels clockwise around the boundary, or equivalently as a chord diagram, connecting the $2n$ points represented on the boundary of a disk via n non-intersecting lines or chords. We denote by LP_n the set of link patterns on $2n$ points, with cardinality $c_n = (2n)!/((n+1)!n!)$, the n-th Catalan number. For each $\pi \in LP_n$, we may ask what is the total number $A_n(\pi)$ of ASM whose FPL configurations connect the external bonds according to π. Razumov and Stroganov (RS) [3] have conjectured a generic answer to this question: the vector $\Psi_n = (\{A_n(\pi)\}_{\pi \in LP_n})$ is the groundstate eigenvector of the Hamiltonian of the O(1) loop model, acting on link patterns. Many other conjectures have flourished since, involving specific symmetry classes of ASM and variations on the boundary conditions of the O(1) loop model (see [4] and also [5] [6] for a nice review and more conjectures).

In [1], we have been able to mix both types of observables and to find a generalization of the RS conjecture involving the numbers $A_{n,m}(\pi)$ of ASM with link pattern π and with 1 in position m in their first row. In the present note, we reformulate this conjecture in terms of the O(1) loop model on a semi-infinite cylinder, and find that it corresponds to a dislocation in the lattice. By considering the case of more dislocations, we will get other nice conjectures. Another direction of generalization was followed in [7], involving O(1) Hamiltonians with boundary terms, and both approaches look unrelated at first sight.

This note is organized as follows. In Sect.2, we review the RS conjecture in the context of O(1) loop model on a semi-infinite cylinder. Sect.3 is devoted to the reformulation of the refined RS conjecture of [1] in terms of the O(1) loop model on a semi-infinite cylinder with a dislocation. In Sect.4, we extend this conjecture to a relation between the two-dislocation O(1) loop model and the doubly-refined ASM numbers in which the positions

of the 1's in both top and bottom rows of the matrices are recorded. Sect.5 is concerned with the m-dislocation case, which produces new numbers awaiting a good combinatorial interpretation. We gather a few concluding remarks in Sect.6.

2. RS conjecture in terms of the O(1) loop gas on a semi-infinite cylinder

2.1. The model and its geometrical setting

We consider a semi-infinite cylinder of (curved) square lattice, with a boundary of perimeter $2n$. The configurations of the O(1) loop gas are simply generated by filling each square face of the lattice by either of the two local loop configurations  or  , say with weights t and $1-t$ respectively. Indeed, this results in drawing non-intersecting loops passing by the centers of the edges of the lattice, with a fugacity $n = 1$ per loop here.

For a given configuration, the centers of the boundary edges, labeled $1, 2, ..., 2n$ in clockwise direction, are pairwise connected by lines of the loop model, according to a link pattern $\pi \in LP_n$.

2.2. Transfer matrix and Hamiltonian

The configurations of the O(1) loop model are generated by a row-to-row transfer matrix $T(t)$ including the abovementioned weights, and with periodic boundary conditions around the cylinder. The matrix $T(t)$ has a nice representation in a basis indexed by link patterns, using the Cyclic Temperley-Lieb algebra generators $e_1, e_2, ..., e_{2n}$. The generator e_i acts on a link pattern π as follows: assume the point i is connected to j and $i+1$ to k in π, then $e_i\pi$ is identical to π except that now j is connected to k and i to $i+1$. Note that this is done without introducing any crossing between chords. The generators satisfy the relations $e_i^2 = e_i$ and $e_i e_{i\pm1} e_i = e_i$ with the convention that $e_{2n+1} \equiv e_1$. Introducing the face transfer matrix operator

$$X_i(t) = tI + (1-t)e_i \tag{2.1}$$

$T(t)$ is nothing but a product of X's, and the periodic boundary condition amounts to a trace over an auxiliary space, as displayed in Fig.2.

Thanks to the Yang-Baxter relation satisfied by the Boltzmann weights of the model, itself a consequence of the Temperley-Lieg algebra relations satisfied by the e_i's, transfer matrices at two distinct values of t commute, hence they share the same eigenvectors, in

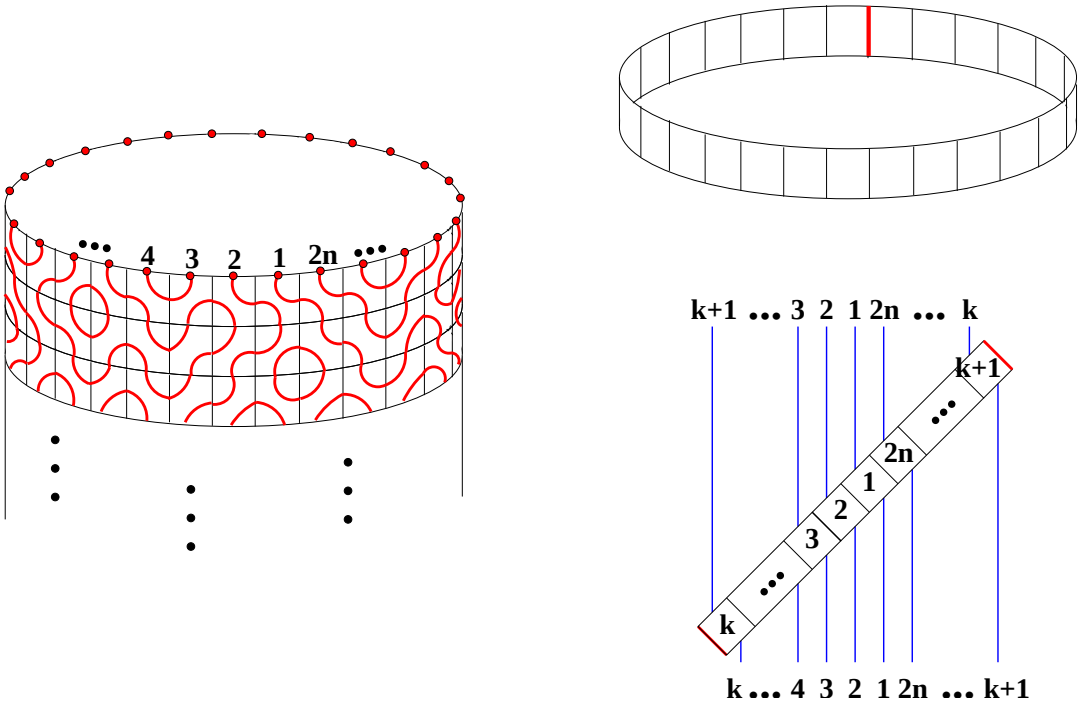

Fig. 2: Typical configuration of the O(1) loop gas on a semi-infinite cylinder. We have isolated the transfer matrix adding an extra row to the cylinder, and pictured it in terms of face transfer matrix operators $X_i(t)$, represented as (tilted) squares 

. The last picture involves a gluing along thick red edges, corresponding to a trace over an auxiliary space.

particular the same Perron-Frobenius eigenvector (for $0 < t < 1$), with maximal eigenvalue and all entries positive.

Interpreting the factor t as a probability, let $\Psi_n(\pi)$ denote the probability in random configurations of the O(1) loop model (obtained by taking independently on each square face the weight  with probability t and  with probability $1-t$), that boundary points of the semi-infinite cylinder be connected according to a given link pattern π. These quantities may be viewed as the components of a vector $\Psi_n = \left(\{\Psi_n(\pi)\}_{\pi\in LP_n}\right)^t$ in the above link pattern basis. This vector is easily seen to satisfy

$$T_n(t)\Psi_n = \Psi_n \tag{2.2}$$

obtained by adding an extra row to the semi-infinite cylinder, and using the action of $T_n(t)$ on link patterns: this simply expresses that adding a row to the semi-infinite cylinder leaves the probabilities invariant. This shows that Ψ_n is the Perron-Frobenius eigenvector

of $T_n(t)$, independent of t. Expanding $T_n(t)$ around $t = 1^-$, one gets the following null-vector equation:

$$H_n \Psi_n = 0 \tag{2.3}$$

where

$$H_n = \sum_{i=1}^{2n} (I - e_i) \tag{2.4}$$

is the Hamiltonian of the model.

2.3. RS conjecture

The RS conjecture involves a suitably normalized version of Ψ_n, in which all the entries are minimal positive integers, rather than fractions summing to 1 in the case of probabilities. By a slight abuse of notation, we still denote this vector by Ψ_n. Another characterization is that $\Psi_n(\pi_0) = 1$ for the "parallel" link pattern $\pi_0 \equiv (2,1)(n+2, n+1)(n+3, n)...(2n, 3)$. Razumov and Stroganov [3] conjectured that the normalized entries $\Psi_n(\pi)$ simply count the number of FPL configurations on a $n \times n$ grid, paired according to the *same* link pattern π.

A by-product of the RS conjecture is that the sum of entries of Ψ_n should equal the total number A_n (1.1) of ASM of size $n \times n$, namely

$$v_n \Psi_n = A_n \tag{2.5}$$

where $v_n = (1, 1, 1..., 1)$.

3. First refinement: O(1) loop gas on a semi-infinite cylinder with a dislocation

3.1. Geometrical setting

We consider the O(1) loop model on a semi-infinite cylinder of square lattice after implementing an elementary dislocation (shift of one lattice spacing) along an infinite line perpendicular to the boundary, as shown in Fig.3. This is represented as an indentation along the boundary, whose edge centers are labeled $1, 2, ..., 2n$ in clockwise direction, the label 1 being attached to the "dislocated" edge as shown. In any given O(1) loop model configuration, these $2n$ points are paired according to a link pattern π.

Like in Sect.2.2, we consider the probability $\Psi_n^{(1)}(\pi|t)$ that a random configuration of the loop model connects the boundary points according to the link pattern $\pi \in LP_n$.

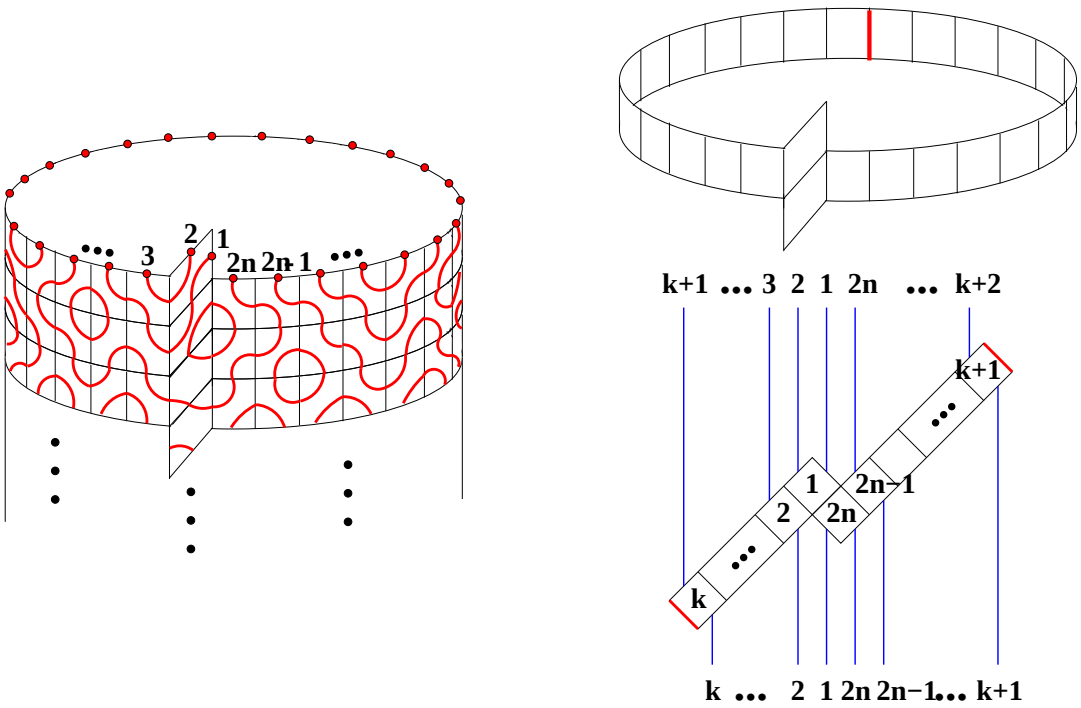

Fig. 3: Typical configuration of the O(1) loop gas on a semi-infinite cylinder with a dislocation, resulting in an indentation of the boundary. We have isolated the transfer matrix adding an extra row to the picture, and represented it pictorially in terms of face transfer matrix operators $X_i(t)$ (2.1) as before.

3.2. Transfer matrix and refined RS conjecture

The configurations of the model may be generated by use of a transfer matrix $T_n^{(1)}(t)$, which corresponds to adding a "row" to the picture, as shown in Fig.3. This matrix is expressed simply as

$$T_n^{(1)}(t) = X_1(t)X_2(t)...X_{2n}(t) \tag{3.1}$$

as should be clear from Fig.3 (the trace over the auxiliary space, indicated by the thick red line, is now an ordinary contraction in the product of the X's). Forming again a vector $\Psi_n^{(1)}(t) = \left(\{\Psi_n^{(1)}(\pi|t)\}_{\pi\in LP_n}\right)^t$, we obtain the Perron-Frobenius eigenvector equation

$$T_n^{(1)}(t)\Psi_n^{(1)}(t) = \Psi_n^{(1)}(t) \tag{3.2}$$

expressing that adding a row to the indented semi-infinite cylinder does not affect the probabilities. Note that v_n is the left Perron-Frobenius eigenvector of $T_n^{(1)}(t)$ with same eigenvalue 1, due to $v_n e_i = v_n$ (as e_i sends any link pattern to another one) and hence

$v_n X_i(t) = X_i(t)$ for all i. In [1], picking a normalization in which $\Psi_n^{(1)}(\pi_0|t) = 1$, it was conjectured that all entries $\Psi_n^{(1)}(\pi|t)$ are polynomials of t with degree $\leq n-1$, and that

$$v_n \Psi_n^{(1)}(t) = \sum_{m=1}^{n} A_{n,m} t^{m-1} \tag{3.3}$$

the generating function for the numbers $A_{n,m}$ ASM with a 1 at a fixed position m in their top row (1.2).

Introducing the clockwise rotation of link patterns

$$\begin{aligned} &r: \ i \to i+1 \qquad \text{for } i = 1, 2, ..., 2n-1 \\ &r: \ 2n \to 1 \end{aligned} \tag{3.4}$$

it was also found that for each link pattern π, the sums $\sum_{m=0}^{\ell(\pi)-1} \Psi_n(r^m \pi|t)$, $\ell(\pi)$ the smallest positive integer ℓ such that $r^\ell \pi = \pi$, are nothing but the generating functions of FPL configurations with a fixed position of the crossing vertex in their top row, and with connectivities given by π up to rotations.

3.3. A family of commuting operators

The rotation r (3.4) of link patterns introduced above satisfies the relations $re_i = e_{i-1}r$ for all i, and therefore $rX_i(t) = X_{i-1}(t)r$. Introducing the operators

$$U_i(t) = r^i X_{2n+1-i}(t) X_{2n+2-i}(t) \cdots X_{2n}(t) \tag{3.5}$$

we immediately get that

$$U_i(t) U_j(t) = U_j(t) U_i(t) = U_{i+j}(t) \tag{3.6}$$

by commuting the r's all the way to the left. So all the U's commute with each other and in particular, $U_{2n}(t) = T_n^{(1)}(t)$ commutes with $U_1(t) = rX_{2n}(t)$, therefore these two operators share the same Perron-Frobenius eigenvector $\Psi_n^{(1)}(t)$. This provides us with an alternative characterization of $\Psi_n^{(1)}(t)$ via

$$U_1(t) \Psi_n^{(1)}(t) = \Psi_n^{(1)}(t) \quad \Leftrightarrow \quad H_n^{(1)}(t) \Psi_n^{(1)}(t) = 0 \tag{3.7}$$

where

$$H_n^{(1)}(t) = I - r^{-1} + (t-1)(I - e_{2n}) \tag{3.8}$$

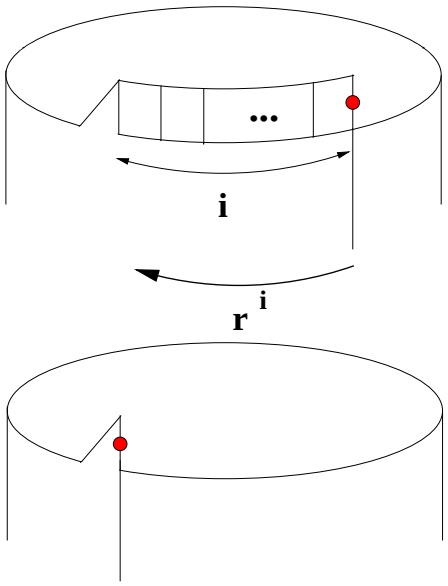

Fig. 4: The action with $U_i(t)$ of (3.5) on configurations of the O(1) loop model on a semi-infinite cylinder. Top: the product of X's adds up i squares to the boundary, thus shifting the indentation by i lattice spacings (the edge of the new dislocation is marked by a red dot). Bottom: the operator r^i shifts the indentation back to the initial position (red dot). The boundary and therefore the probabilities of the model are left invariant in the process.

The latter looks much simpler than $T_n^{(1)}(t) - I$, in particular it is linear in t.

The fact that $U_i(t)\Psi_n^{(1)}(t) = \Psi_n^{(1)}(t)$ for all i may be understood directly from a geometrical point of view, as shown in Fig.4. The multiplication by $X_{2n+i-i}(t)...X_{2n}(t)$ amounts to adding a row of i consecutive squares to the semi-infinite cylinder, from some position down to the indentation. This has the net effect of shifting the indentation of the boundary by i lattice spacings. Finally, the operator r^i rotates back the picture in such a way that the indentation gets back to the initial position: the probabilities, and therefore $\Psi_n^{(1)}(t)$, are clearly invariant in the process.

4. Second refinement: O(1) loop gas on a semi-infinite cylinder with two dislocations

4.1. Geometrical setting

Inspired by the interpretation of Sect.3, we now consider the O(1) loop model on a semi-infinite cylinder of square lattice with $2n$ boundary edges, and with *two* elementary

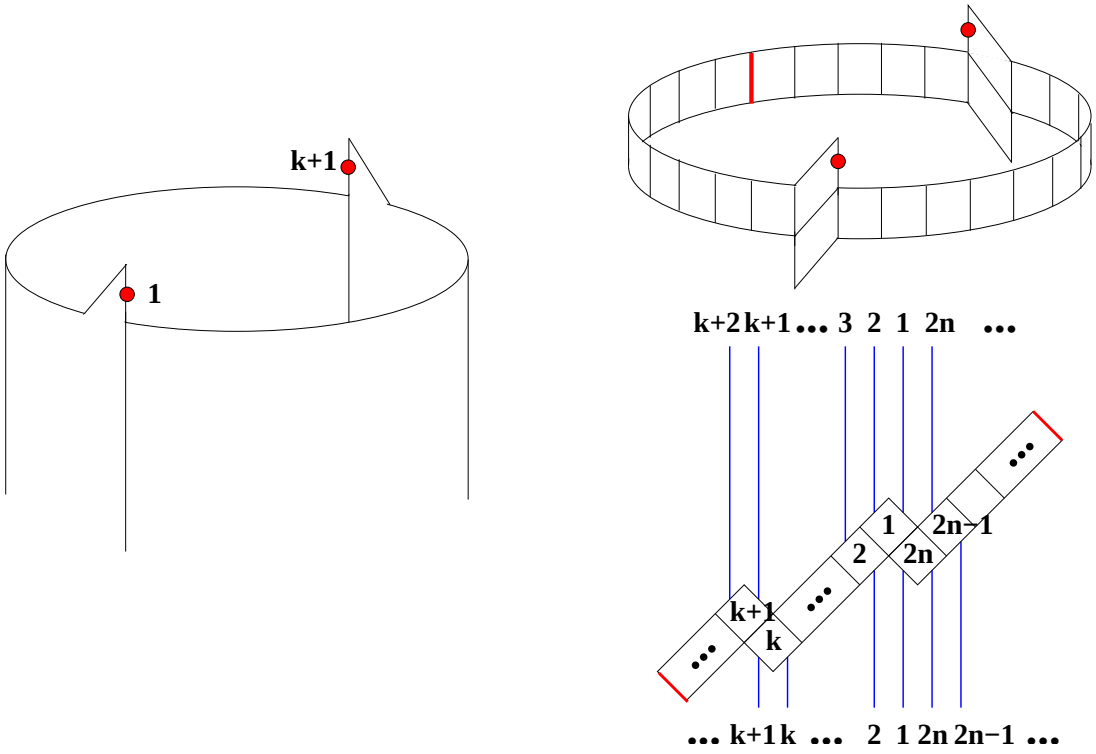

Fig. 5: A typical "two-dislocation" boundary condition on the semi-infinite cylinder. The transfer matrix is shown and then decomposed into a product of $X_i(t)$ operators as before.

dislocations, as shown in Fig.5, say with dislocated edges labeled 1 and $k+1$. We denote by $\Psi_n^{(1,k+1)}(\pi|t)$ the probability that a random O(1) loop model configuration on this semi-infinite cylinder connects the boundary points according to the link pattern $\pi \in LP_n$.

4.2. Transfer matrix, Perron-Frobenius eigenvector and a first conjecture

It is easy to read off Fig.5 the following transfer matrix $T_n^{(1,k+1)}(t)$ that adds up a row to the semi-infinite cylinder with two dislocations:

$$T_n^{(1,k+1)}(t) = X_{k+1}(t)X_1(t)X_2(t)...X_k(t)X_{k+2}(t)X_{k+3}(t)...X_{2n}(t) \tag{4.1}$$

and the vector $\Psi_n^{(1,k+1)}(t) = \{\Psi_n^{(1,k+1)}(\pi|t)\}_{\pi\in LP_n}$ is nothing but the Perron-Frobenius eigenvector of $T_n^{(1,k+1)}(t)$:

$$T_n^{(1,k+1)}(t)\Psi_n^{(1,k+1)}(t) = \Psi_n^{(1,k+1)}(t) \tag{4.2}$$

Like in Sect.3.3, we may drastically simplify the eigenvector equation (4.2) by noticing that we may replace $T_n^{\{1,k\}}(t)$ with any of the operators

$$U_i^{(1,k+1)}(t) = r^i X_{2n+1-i}(t)X_{k+1-i}(t)X_{2n+2-i}(t)X_{k+2-i}(t)...X_{2n}(t)X_k(t) \tag{4.3}$$

which simply add up successively i consecutive pairs of squares, one after each of the two indentations, thus shifting both of them by i lattice spacings, and then takes them both to their original positions by the global rotation r^i. As in Sect.3.3, we find that all these operators commute with each other as $U_i^{(1,k+1)}(t)U_j^{(1,k+1)}(t) = U_{i+j}^{(1,k+1)}(t)$, and they all leave the probabilities invariant. Note that none of the $U_i^{\{1,k\}}(t)$ is actually equal to the transfer matrix $T_n^{(1,k+1)}(t)$, as opposed to the case of Sect.3.3, although they do commute with it. The simplest of all equations obeyed by $\Psi_n^{(1,k+1)}(t)$ reads

$$U_1^{(1,k+1)}(t)\Psi_n^{(1,k+1)}(t) = \Psi_n^{(1,k+1)}(t) \quad \Leftrightarrow \quad H_n^{(1,k+1)}(t)\Psi_n^{(1,k+1)}(t) = 0 \tag{4.4}$$

where

$$H_n^{(1,k+1)}(t) = X_k(t)X_{2n}(t) - r^{-1} = I - r^{-1} + (1-t)(e_k + e_{2n} - 2I) + (1-t)^2(e_k - I)(e_{2n} - I) \tag{4.5}$$

It is simply quadratic in t.

A direct computation of the first few $\Psi_n^{(1,k+1)}(t)$ has led us to the following conjecture. With a suitable normalization described below, the sum of the components of $\Psi_n^{(1,k+1)}(t)$ is a polynomial of degree $2(n-1)$ with only non-negative integer coefficients, independent of $k \in \{2, 3, ..., 2n-2\}$. This polynomial coincides with the generating function for the numbers of ASM with fixed sum of the positions of their 1's in the top and bottom row. More precisely, let $A_{n,m,p}$ denote the total number of ASM with a 1 in position m (counted from the left) in the top row and a 1 in position p (counted from the right) in the bottom row[1], then we have

$$v_n\Psi_n^{(1,k+1)}(t) = \sum_{m,p=1}^{n} A_{n,m,p}t^{m+p-2} \tag{4.6}$$

That this quantity is independent of k is a direct consequence of the fact that v_n is a left eigenvector of all the X's with eigenvalue 1, namely $v_nX_i(t) = v_n$ for all i. Indeed, for $l < k$, we have $\Psi_n^{(1,l+1)}(t) = X_{l+1}(t)X_{l+2}(t)...X_k(t)\Psi_n^{(1,k+1)}(t)$ for the vectors of probabilities, where the indentation in position $k+1$ has been shifted by $k-l$ lattice spacings counterclockwise, and therefore $v_n\Psi_n^{(1,l+1)}(t) = v_n\Psi_n^{(1,k+1)}(t)$. The normalization of all the Ψ's is then fixed by that of $\Psi_n^{(1,n+1)}(t)$, in which we fix $\Psi_n^{(1,n+1)}(\pi_0|t) = 1$. With this choice, it turns out that all the components of $\Psi_n^{(1,n+1)}(t)$ are polynomials of t of degree $\leq 2n-2$, with only non-negative integer coefficients, and summing to (4.6).

[1] These numbers are displayed in appendix A up to $n = 6$, via the generating polynomials $A_n(t,u) = \sum_{m,p=1}^{n} A_{n,m,p}t^{m-1}u^{p-1}$. As opposed to the refined ASM numbers (1.2), these doubly-refined numbers do not seem to have any nice product form. As an example, the ASM of Fig.1 (a) contributes by 1 to $A_{6,5,6} = 105$ (coefficient of t^4u^5 in $A_6(t,u)$ of eq.(A.1)), as the 1 in its bottom row sits in position 6 counted from the right.

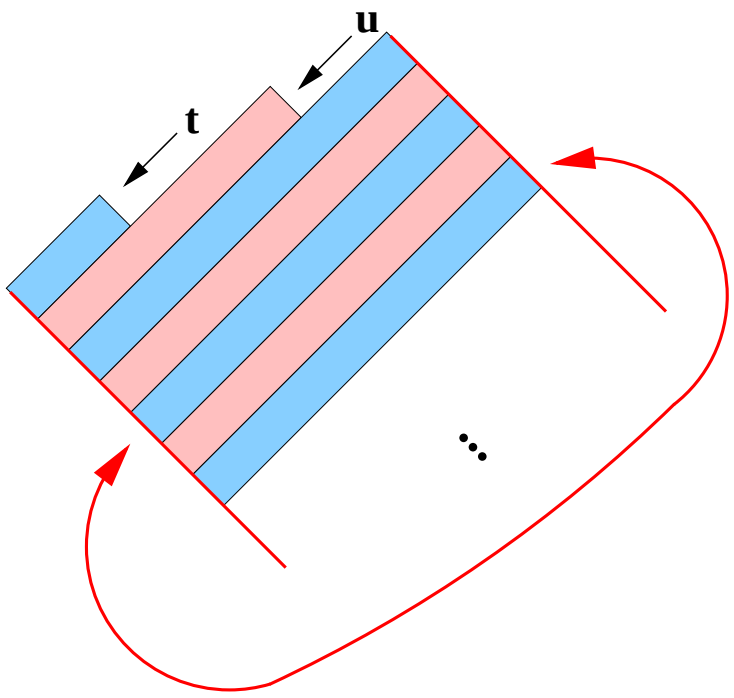

Fig. 6: The double-helix decomposition of the two-dislocation semi-infinite cylinder of square lattice (glued here along the thick red line as indicated). Blue strips correspond to drawing the two possible face loop configurations with probabilities t and $1-t$, while pink strips correspond to probabilities u and $1-u$.

4.3. Doubly refined RS conjecture

The result of the previous section suggests to look for a further refinement of the RS conjecture, allowing for recovering the doubly-refined ASM numbers $A_{n,m,p}$ individually in the context of the O(1) loop model. This is done as follows. Keeping the geometry of the cylinder as in Sect.4.1, we consider an inhomogeneous random O(1) loop model in which the loop configurations  and  , are drawn with probabilities t and $1-t$ respectively on certain faces of the lattice, and u and $1-u$ on others. We actually decompose the two-dislocation semi-infinite cylinder of square lattice, according to Fig.6, into a double-helix formed with one strip of each kind of face.

As before, assuming that the two indentations are in positions 1 and $k+1$, we denote by $\Psi_n^{(1,k+1)}(\pi|t,u)$ the probability that a random configuration of this inhomogeneous O(1) model connects the boundary points according to the link pattern π, and we form the vector $\Psi_n^{(1,k+1)}(t,u) = \left(\{\Psi_n^{(1,k+1)}(\pi|t,u)\}_{\pi\in LP_n}\right)^t$. The transfer matrix for the model must involve the addition of $4n$ squares (and make two complete turns), however the vector

$\Psi_n^{(1,k+1)}(t,u)$ is invariant under the action of the operators

$$U_i^{(1,k+1)}(t,u) = r^i X_{k+1-i}(u) X_{2n+1-i}(t) X_{k+2-i}(u) X_{2n+2-i}(t) ... X_k(u) X_{2n}(t) \qquad (4.7)$$

for all i, so we may write the simplest of the corresponding Perron-Frobenius equations $U_1^{(1,k+1)}(t,u)\Psi_n^{(1,k+1)}(t,u) = \Psi_n^{(1,k+1)}(t,u)$, or equivalently

$$H_n^{(1,k+1)}(t,u)\Psi_n^{(1,k+1)}(t,u) = 0 \qquad (4.8)$$

with

$$H_n^{(1,k+1)}(t,u) = I - r^{-1} + (1-t)(e_{2n}-I) + (1-u)(e_k - I) + (1-t)(1-u)(e_k-I)(e_{2n}-I) \quad (4.9)$$

This operator is simply linear in each of the variables t, u. Note that when $u = 1$ (4.9) reduces to (4.5). We have computed the first few $\Psi_n^{(1,k+1)}(t,u)$ by use of eqs.(4.8)-(4.9). The results have suggested the following conjecture.

Picking a normalization in which $\Psi_n^{(1,n+1)}(\pi_0|t,u) = 1$, the entries of $\Psi_n^{(1,n+1)}(t,u)$ are all polynomials of t, u of degree $\leq n-1$ in each variable, with only non-negative integer coefficients. Moreover the sum of entries is nothing but the generating function for ASM with 1's in fixed positions on their top and bottom row:

$$v_n \Psi_n^{(1,n+1)}(t,u) = \sum_{m,p=0}^{n-1} A_{n,m,p} t^{m-1} u^{p-1} \qquad (4.10)$$

The vectors $\Psi_n^{(1,n+1)}(t,u)$ are listed in appendix B up to $n = 5$, while the generating polynomials for ASM with 1's in fixed positions on their top and bottom row are listed in appendix A up to $n = 6$.

We have not been able to relate directly the components of $\Psi_n^{(1,n+1)}(t,u)$ to FPL configurations with fixed connectivity and positions of crossing vertices in their top and bottom rows.

Noticing again that we may sweep all the vectors $\Psi_n^{(1,k+1)}(t,u)$ upon acting with X's on any of them, we find that eq.(4.10) holds for any $\Psi_n^{(1,k+1)}(t,u)$, for $k = 2, 3, ..., 2n-2$, although entries are no longer necessarily polynomials with non-negative integer coefficients. The case $k = n$ is singled-out as corresponding to the only "self-reflected" boundary, namely allowing for a gluing between the original semi-infinite cylinder and its reflection, into an infinite cylinder expressed as a glued infinite double-helix of the two types of faces.

5. Multiple refinements: O(1) loop gas on a semi-infinite cylinder with arbitrarily many dislocations

The results of Sect.4 lead to the following straightforward generalization. We now consider a semi-infinite cylinder with m dislocations ($m \leq n$), with m indented boundary edges labeled $1, k_1+1, k_1+k_2+1, ..., k_1+k_2+...+k_{m-1}+1$ clockwise. Taking uniform probabilities t and $1-t$ for the two possible O(1) loop face configurations, we denote by $\Psi_n^{(\{k\})}(\pi|t) \equiv \Psi_n^{(1,k_1+k_2+...+k_{m-1}+1,k_1+k_2+...+k_{m-2}+1,...,k_1+1)}(\pi|t)$ the probability that a random configuration of the O(1) loop model connects the boundary points according to the link pattern $\pi \in LP_n$.

As before, we readily get the simplest Perron-Frobenius equation for the vector $\Psi_n^{(\{k\})}(t) = \left(\{\Psi_n^{(\{k\})}(\pi|t)\}_{\pi \in LP_n}\right)^t$

$$U_1^{(\{k\})}(t)\Psi_n^{(\{k\})}(t) = \Psi_n^{(\{k\})}(t) \tag{5.1}$$

by acting with the operator

$$U_1^{(\{k\})}(t) = rX_{k_1+k_2+...+k_{m-1}}(t)X_{k_1+k_2+...+k_{m-2}}(t)...X_{k_1}(t)X_{2n}(t) \tag{5.2}$$

which shifts all m indentations by one lattice spacing and then takes them back to their original position via a global clockwise rotation r. The operator (5.2) has degree m in t. Using eqs.(5.1)-(5.2), we have computed the first few vectors Ψ, and the results have suggested the following conjecture.

As before, with a suitable normalization of the Ψ's, the sum of entries $P_n(m|t) \equiv v_n\Psi_n^{(\{k\})}(t)$ is independent of the k_i's, provided they are all ≥ 2, and it is a polynomial of degree $nm - [\frac{m^2+1}{2}]$ of t, with only non-negative integer coefficients. Moreover, some specific choices of the k's (those which best spread the positions of the indentations around the boundary, and correspond like in Sect.4.3 to "self-reflected" half-cylinder boundaries) yield Ψ's whose entries are all polynomials of t with only non-negative integer coefficients, but we have not been able to relate directly the components of these Ψ's to specific classes of FPL configurations. In particular, when the number of dislocations is maximal ($m = n$) and all $k_i = 2$, we find that all the entries of Ψ are polynomials of degree $\leq [\frac{n^2}{2}]$ with non-negative integer coefficients. The first few $P_n(m|t)$'s for $1 \leq m \leq n \leq 6$ are listed in appendix C below.

By construction, we have $P_n(m|t=1) = A_n$ the total number of FPL or ASM of size $n \times n$. We may therefore expect that the polynomials $P_n(m|t)$ yield decompositions of these

numbers according to some properties of the corresponding ASM or FPL configurations. In Sects.3.2 and 4.2, we have found such interpretations for $P_n(1|t)$ and $P_n(2|t)$ respectively.

Our attempts to decorate the m-dislocation case with different probabilities corresponding to multiple helix decompositions of the semi-infinite cylinder have not led us to any nice multi-variable polynomial generalizations of $P_n(m|t)$: it seems that the two-variable generalizations (4.10) are the best we can do.

6. Conclusion and discussion

6.1. RS conjectures and the ASM/FPL–TSSCPP correspondence

In this note we have extended the refined RS conjecture of [1] by rephrasing it in terms of the O(1) loop model on a semi-infinite cylinder. This has led to other generalizations in which we consider a cylinder with defects (dislocations), translating into indentations on the boundary. The classical RS conjecture corresponds to the case of no dislocation. The refined RS conjecture of [1] corresponds to the case of one dislocation.

By decorating the two-dislocation case with two types of probability weights corresponding to a decomposition of the cylinder into a double-helix, we have found that the sum of entries of the suitably renormalized probability vector of the model could be identified with the generating function for doubly-refined ASM numbers, namely the numbers of ASM with both positions of their 1's in the top and bottom row specified. These numbers were already referred to in [8] in the context of the (still mysterious) relation between ASM and totally-symmetric self-complementary plane partitions (TSSCPP). More precisely, the generating functions for TSSCPP with both numbers f_2 and f_3 fixed (c.f. [8] for definitions) also coincide with our polynomials $v_n \Psi_n^{(1,n+1)}(t,u)$. Our two-dislocation conjecture may be a first step toward a more precise connection between all these counting problems. Actually, it might be that the apparent mismatch between the entries $\Psi_n^{(1,n+1)}(\pi|t,u)$ and the doubly-refined ASM number generating functions with fixed connectivity π, $\sum_{m,p} A_{n,m,p}(\pi) t^{m-1} u^{p-1}$, even up to rotations of π, simply means that we have not yet understood the correct ASM picture corresponding to $\Psi_n^{(1,n+1)}(t,u)$. In particular, in [8], Robbins describes three numbers f_1, f_2, f_3 attached to each TSSCPP, any pair of which have the same distribution within TSSCPP as the $A_{n,m,p}$ within ASM. If we believe in the existence of a natural ASM-TSSCPP bijection, we see that a third observable is clearly missing in the ASM picture to account for the triplet f_1, f_2, f_3. This

third observable is perhaps the missing link between our vector $\Psi_n^{(1,n+1)}(t,u)$ and (triply?) refined ASM with fixed connectivities.

In addition, we have been able to produce more non-negative integer numbers out of the m-dislocation case, which, we hope, should have an interpretation in both ASM and TSSCPP contexts.

6.2. Open case

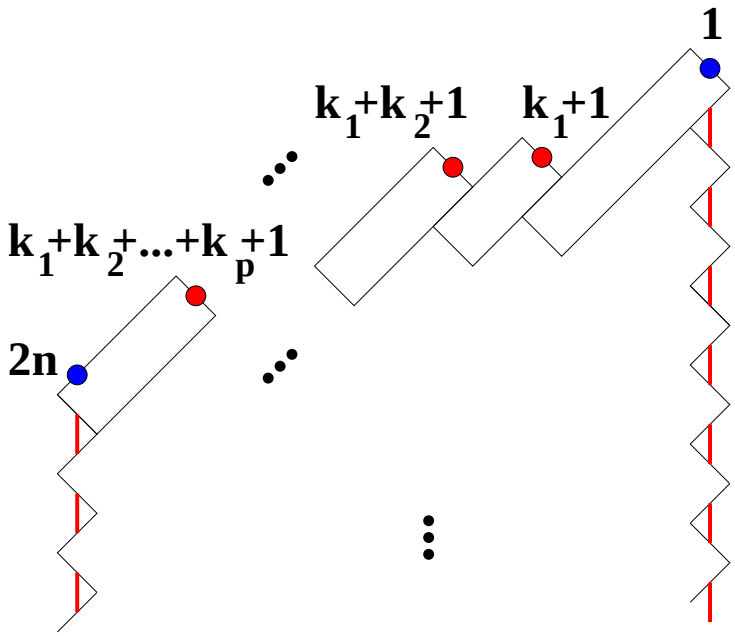

Fig. 7: O(1) model on a semi-infinite strip of width $2n$ (open cylinder), with p indentations on the boundary (red dots). The corresponding transfer matrix is decomposed into strips of tilted squares, corresponding to multiplication by operators $X_i(t)$.

The conjectures of this paper have a natural extension in the open (or semi-infinite strip) case, where we draw an impenetrable half-line along the cylinder that separates the points 1 and $2n$ of the boundary, thus transforming the domain into a semi-infinite strip of width $2n$. Going directly to the most general situation of a boundary with p indentations in positions $\{k\} \equiv k_1+1, k_1+k_2+1, \cdots, k_1+k_2+\cdots+k_p+1$ (see Fig.7), and introducing the probabilities $\Psi_{2n}^{O\,\{k\}}(\pi|t)$ that a random homogeneous O(1) loop model configuration connects the boundary points according to the link pattern $\pi \in LP_n$, we get the eigenvector equation

$$T_{2n}^{O\,\{k\}}(t)\Psi_{2n}^{O\,\{k\}}(t) = \Psi_{2n}^{O\,\{k\}}(t) \tag{6.1}$$

expressing the invariance of the probabilities under addition of a layer of squares parallely to the boundary, via the transfer matrix

$$\begin{aligned} T_{2n}^{O\,\{k\}}(t) &= X_{k_1+\ldots+k_p+1}(t)X_{k_1+\ldots+k_{p-1}+1}(t)\ldots X_{k_1+1}(t) \times X_1(t)X_2(t)\ldots X_{k_1}(t) \\ &\times X_{k_1+2}(t)X_{k_1+3}(t)\ldots X_{k_1+k_2}(t) \times \ldots \times X_{k_1+\ldots+k_p+2}(t)X_{k_1+\ldots+k_p+3}(t)\ldots X_{2n}(t) \end{aligned} \tag{6.2}$$

The computation of the first few Ψ^O's has led us to the following conjecture.

Noting that all the eigenvectors $\Psi_{2n}^{O\,\{k\}}(t)$ at different values and numbers of k's are all related to one-another via products of X's, we find that in a suitable global normalization of all these vectors, the sum of entries

$$P_{2n}^O(t) = v_n \Psi_{2n}^{O\,\{k\}}(t) \tag{6.3}$$

is a polynomial of t independent of p and the k's, of degree $n(n-1)$ and with only non-negative integer coefficients.

This is readily extended to the case of a strip of width $2n-1$, by simply removing the factor $X_{2n}(t)$ in the definition of $T_{2n}^{O\,\{k\}}(t) \to T_{2n-1}^{O\,\{k\}}(t)$. The conjecture above becomes that in a suitable normalization, the sum of eigenvector entries

$$P_{2n-1}^O(t) = v_n \Psi_{2n-1}^{O\,\{k\}}(t) \tag{6.4}$$

is a polynomial of t independent of p and the k's, of degree $(n-1)^2$ and with only non-negative integer coefficients.

The polynomials $P_m^O(t)$ are listed in appendix D, up to $m = 10$. Note that according to the classical RS conjectures for the open case [9], $P_{2n}^O(t=1)$ is the total number $A_V(2n+1)$ of vertically-symmetric ASM/FPL of size $(2n+1) \times (2n+1)$, while $P_{2n-1}^O(t=1)$ is the total number $N_8(2n)$ of cyclically-symmetric transpose-complement plane partitions in a box of size $2n \times 2n \times 2n$. The polynomials $P_m^O(t)$ form respective refinements of these numbers, which still await some good combinatorial interpretation.

Acknowledgments

We thank E. Guitter, C. Krattenthaler and J.-B. Zuber for their help at different stages of this work.

Appendix A. Polynomials generating the numbers of ASM with fixed positions of 1's in their top and bottom row

We list below up to $n = 6$ the polynomials $A_n(t,u) = \sum_{m,p=1}^{n} A_{n,m,p} t^{m-1} u^{p-1}$, which generate the numbers $A_{n,m,p}$ of ASM with 1's in their top and bottom rows respectively sitting at positions m and p counted from left (top) and right (bottom). These were computed by transfer matrix techniques on the FPL model.

$$
\begin{aligned}
A_1(t,u) &= 1 \\
A_2(t,u) &= 1 \\
&\quad + tu \\
A_3(t,u) &= 1 + t \\
&\quad + u + tu + t^2u \\
&\quad + tu^2 + t^2u^2 \\
A_4(t,u) &= 2 + 3t + 2t^2 \\
&\quad + 3u + 5tu + 4t^2u + 2t^3u \\
&\quad + 2u^2 + 4tu^2 + 5t^2u^2 + 3t^3u^2 \\
&\quad + 2tu^3 + 3t^2u^3 + 2t^3u^3 \\
A_5(t,u) &= 7 + 14t + 14t^2 + 7t^3 \\
&\quad + 14u + 30tu + 33t^2u + 21t^3u + 7t^4u \\
&\quad + 14u^2 + 33tu^2 + 41t^2u^2 + 33t^3u^2 + 14t^4u^2 \\
&\quad + 7u^3 + 21tu^3 + 33t^2u^3 + 30t^3u^3 + 14t^4u^3 \\
&\quad + 7tu^4 + 14t^2u^4 + 14t^3u^4 + 7t^4u^4 \\
A_6(t,u) &= 42 + 105t + 135t^2 + 105t^3 + 42t^4 \\
&\quad + 105u + 275tu + 375t^2u + 322t^3u + 168t^4u + 42t^5u \\
&\quad + 135u^2 + 375tu^2 + 547t^2u^2 + 518t^3u^2 + 322t^4u^2 + 105t^5u^2 \\
&\quad + 105u^3 + 322tu^3 + 518t^2u^3 + 547t^3u^3 + 375t^4u^3 + 135t^5u^3 \\
&\quad + 42u^4 + 168tu^4 + 322t^2u^4 + 375t^3u^4 + 275t^4u^4 + 105t^5u^4 \\
&\quad + 42tu^5 + 105t^2u^5 + 135t^3u^5 + 105t^4u^5 + 42t^5u^5
\end{aligned}
\tag{A.1}
$$

Appendix B. Perron-Frobenius vectors for the two-dislocation inhomogeneous O(1) loop model

We list below the vectors $\Psi_n(t,u) \equiv \Psi_n^{(1,n+1)}(t,u)$, computed by solving eq.(4.8), up to $n = 5$. Like in [1], the entries are listed in lexicographic order on the link patterns.

$$
\begin{aligned}
&\Psi_1(t,u) = \{1\}\\
&\Psi_2(t,u) = \{1, tu\}\\
&\Psi_3(t,u) = \{u(1+tu), 1, tu, t(1+tu), t^2u^2\}\\
&\Psi_4(t,u) = \{1+t+u+tu+t^2u+tu^2+t^2u^2, u(1+t+tu), u^2(1+tu+t^2u), u(1+u+tu^2),\\
&1, t(1+u+tu), tu, tu^2(1+t+tu), tu(1+t+u+tu+t^2u+tu^2+t^2u^2), t(1+t+t^2u),\\
&t^2u^2, t^2u(1+u+tu), t^2(1+tu+tu^2), t^3u^3\}\\
&\Psi_5(t,u) = \{u(2+3t+2t^2+3u+5tu+4t^2u+2t^3u+2u^2+4tu^2+5t^2u^2+3t^3u^2+2tu^3+3t^2u^3\\
&+2t^3u^3), u^2(2+3t+2t^2+u+3tu+3t^2u+tu^2+2t^2u^2), 2+3t+2t^2+u+2tu+2t^2u\\
&+2t^3u+tu^2+t^2u^2+t^3u^2, 1+2t+2u+4tu+2t^2u+2tu^2+t^2u^2, u(1+2t+tu),\\
&u(1+t+t^2+2u+2tu+2t^2u+t^3u+2tu^2+3t^2u^2+2t^3u^2), u^2(1+t+t^2+tu+2t^2u),\\
&1+t+t^2+u+tu+t^2u+t^3u+u^2+tu^2+t^2u^2+t^3u^2+tu^3+t^2u^3+t^3u^3,\\
&2+t+3u+2tu+t^2u+2u^2+2tu^2+t^2u^2+2tu^3+t^2u^3, u(2+t+u+tu+tu^2),\\
&u^3(1+tu+t^2u+t^3u), u^2(1+2u+2tu^2+t^2u^2), u(1+u+u^2+tu^3), 1,\\
&tu(2+t+3u+2tu+t^2u+2u^2+2tu^2+t^2u^2+2tu^3+t^2u^3), tu^2(2+t+u+tu+tu^2),\\
&t(2+t+u+tu+t^2u), t(1+2u+tu), tu, tu(1+2t+2u+4tu+2t^2u+2tu^2+t^2u^2),\\
&tu^2(1+2t+tu), t(1+2t+u+2tu+2t^2u+u^2+2tu^2+3t^2u^2+tu^3+2t^2u^3),\\
&t(2+3t+2t^2+3u+5tu+4t^2u+2t^3u+2u^2+4tu^2+5t^2u^2+3t^3u^2+2tu^3+3t^2u^3+2t^3u^3),\\
&tu(2+3t+2t^2+u+2tu+2t^2u+2t^3u+tu^2+t^2u^2+t^3u^2), tu^3(1+t+t^2+tu+2t^2u),\\
&tu^2(1+t+t^2+2u+2tu+2t^2u+t^3u+2tu^2+3t^2u^2+2t^3u^2), tu(1+t+t^2+u+tu+t^2u\\
&+t^3u+u^2+tu^2+t^2u^2+t^3u^2+tu^3+t^2u^3+t^3u^3), t(1+t+t^2+t^3u), t^2u(1+2u+tu), t^2u^2,\\
&t^2(1+u+tu+u^2+2tu^2), t^2(2+t+3u+3tu+t^2u+2u^2+3tu^2+2t^2u^2), t^2u(2+t+u+tu\\
&+t^2u), t^2u^3(1+2t+tu), t^2u^2(1+2t+2u+4tu+2t^2u+2tu^2+t^2u^2), t^2u(1+2t+u+2tu\\
&+2t^2u+u^2+2tu^2+3t^2u^2+tu^3+2t^2u^3), t^2(1+2t+2t^2u+t^2u^2), t^3u^3, t^3u^2(1+2u+tu),\\
&t^3u(1+u+tu+u^2+2tu^2), t^3(1+tu+tu^2+tu^3), t^4u^4\}
\end{aligned}
\tag{B.1}
$$

Appendix C. Polynomials for the multiple-dislocation O(1) loop model

We list below the polynomials $P_n(m|t)$ obtained by solving eq.(5.1), for $1 \le m \le n \le 6$.

$$
\begin{aligned}
P_1(1|t) &= 1 \\
P_2(1|t) &= 1 + t \\
P_2(2|t) &= 1 + t^2 \\
P_3(1|t) &= 2 + 3t + 2t^2 \\
P_3(2|t) &= 1 + 2t + t^2 + 2t^3 + t^4 \\
P_3(3|t) &= 1 + t + 3t^2 + t^3 + t^4 \\
P_4(1|t) &= 7 + 14t + 14t^2 + 7t^3 \\
P_4(2|t) &= 2 + 6t + 9t^2 + 8t^3 + 9t^4 + 6t^5 + 2t^6 \\
P_4(3|t) &= 1 + 4t + 6t^2 + 10t^3 + 10t^4 + 6t^5 + 4t^6 + t^7 \\
P_4(4|t) &= 1 + 2t + 7t^2 + 6t^3 + 10t^4 + 6t^5 + 7t^6 + 2t^7 + t^8 \\
P_5(1|t) &= 42 + 105t + 135t^2 + 105t^3 + 42t^4 \\
P_5(2|t) &= 7 + 28t + 58t^2 + 80t^3 + 83t^4 + 80t^5 + 58t^6 + 28t^7 + 7t^8 \\
P_5(3|t) &= 2 + 11t + 30t^2 + 52t^3 + 76t^4 + 87t^5 + 76t^6 + 52t^7 + 30t^8 + 11t^9 + 2t^{10} \\
P_5(4|t) &= 1 + 6t + 15t^2 + 34t^3 + 54t^4 + 66t^5 + 77t^6 + 66t^7 + 54t^8 + 34t^9 + 15t^{10} + 6t^{11} + t^{12} \\
P_5(5|t) &= 1 + 4t + 16t^2 + 30t^3 + 55t^4 + 67t^5 + 83t^6 + 67t^7 + 55t^8 + 30t^9 + 16t^{10} + 4t^{11} + t^{12} \\
P_6(1|t) &= 429 + 1287t + 2002t^2 + 2002t^3 + 1287t^4 + 429t^5 \\
P_6(2|t) &= 42 + 210t + 545t^2 + 960t^3 + 1275t^4 + 1372t^5 + 1275t^6 + 960t^7 + 545t^8 + 210t^9 + 42t^{10} \\
P_6(3|t) &= 7 + 49t + 174t^2 + 412t^3 + 730t^4 + 1062t^5 + 1284t^6 + 1284t^7 + 1062t^8 + 730t^9 + 412t^{10} \\
&\quad + 174t^{11} + 49t^{12} + 7t^{13} \\
P_6(4|t) &= 2 + 16t + 64t^2 + 168t^3 + 354t^4 + 608t^5 + 868t^6 + 1064t^7 + 1148t^8 + 1064t^9 + 868t^{10} \\
&\quad + 608t^{11} + 354t^{12} + 168t^{13} + 64t^{14} + 16t^{15} + 2t^{16} \\
P_6(5|t) &= 1 + 9t + 36t^2 + 110t^3 + 255t^4 + 467t^5 + 738t^6 + 972t^7 + 1130t^8 + 1130t^9 + 972t^{10} \\
&\quad + 738t^{11} + 467t^{12} + 255t^{13} + 110t^{14} + 36t^{15} + 9t^{16} + t^{17} \\
P_6(6|t) &= 1 + 6t + 30t^2 + 84t^3 + 204t^4 + 372t^5 + 624t^6 + 828t^7 + 1035t^8 + 1068t^9 + 1035t^{10} \\
&\quad + 828t^{11} + 624t^{12} + 372t^{13} + 204t^{14} + 84t^{15} + 30t^{16} + 6t^{17} + t^{18}
\end{aligned}
\tag{C.1}
$$

Appendix D. Polynomials for the O(1) loop model on a strip of finite width

Up to $m = 10$, the polynomials $P_m^O(t)$ (6.3)-(6.4) read:

$$
\begin{aligned}
P_1^O(t) &= 1 \\
P_2^O(t) &= 1 \\
P_3^O(t) &= 1 + t \\
P_4^O(t) &= 1 + t + t^2 \\
P_5^O(t) &= 1 + 3t + 3t^2 + 3t^3 + t^4 \\
P_6^O(t) &= 1 + 3t + 6t^2 + 6t^3 + 6t^4 + 3t^5 + t^6 \\
P_7^O(t) &= 1 + 6t + 15t^2 + 28t^3 + 35t^4 + 35t^5 + 28t^6 + 15t^7 + 6t^8 + t^9 \\
P_8^O(t) &= 1 + 6t + 21t^2 + 46t^3 + 81t^4 + 108t^5 + 120t^6 + 108t^7 + 81t^8 + 46t^9 + 21t^{10} + 6t^{11} + t^{12} \\
P_9^O(t) &= 1 + 10t + 45t^2 + 140t^3 + 320t^4 + 585t^5 + 886t^6 + 1120t^7 + 1215t^8 + 1120t^9 + 886t^{10} \\
&\quad + 585t^{11} + 320t^{12} + 140t^{13} + 45t^{14} + 10t^{15} + t^{16} \\
P_{10}^O(t) &= 1 + 10t + 55t^2 + 200t^3 + 560t^4 + 1253t^5 + 2345t^6 + 3740t^7 + 5180t^8 + 6260t^9 + 6677t^{10} \\
&\quad + 6260t^{11} + 5180t^{12} + 3740t^{13} + 2345t^{14} + 1253t^{15} + 560t^{16} + 200t^{17} + 55t^{18} + 10t^{19} + t^{20}
\end{aligned}
\tag{D.1}
$$

References

[1] P. Di Francesco, *A refined Razumov-Stroganov conjecture*, JSTAT 2004 P08009, arXiv:cond-mat/0407477.

[2] D. Bressoud, *Proofs and confirmations. The story of the alternating sign matrix conjecture*, Cambridge University Press (1999).

[3] A.V. Razumov and Yu.G. Stroganov, *Combinatorial nature of ground state vector of O(1) loop model*, Theor. Math. Phys. **138** (2004) 333-337, arXiv:math.CO/0104216.

[4] A.V. Razumov and Yu.G. Stroganov, *O(1) loop model with different boundary conditions and symmetry classes of alternating-sign matrices*, arXiv:cond-mat/0108103.

[5] S. Mitra, B. Nienhuis, J. de Gier and M.T. Batchelor, *Exact expressions for correlations in the ground state of the dense $O(1)$ loop model*, arXiv:cond-math/0401245

[6] S. Mitra and B. Nienhuis, *Osculating random walks on cylinders*, in *Discrete random walks*, DRW'03, C. Banderier and C. Krattenthaler edrs, Discrete Mathematics and Computer Science Proceedings AC (2003) 259-264, arXiv:math-ph/0312036 and *Exact conjectured expressions for correlations in the dense O(1) loop model on cylinders*, arXiv:cond-mat/0407578.

[7] J. De Gier and V. Rittenberg, *Refined Razumov-Stroganov conjectures for open boundaries*, arXiv:math-ph/0408042.

[8] D. Robbins, *The story of 1,2,7,42,429,7436,...*, Mathl. Intelligencer **13** No.2 (1991) 12-19.

[9] P. Pearce, V. Rittenberg and J. de Gier, *Critical Q=1 Potts Model and Temperley-Lieb Stochastic Processes*, arXiv:cond-mat/0108051 and A.V. Razumov and Yu.G. Stroganov, *O(1) loop model with different boundary conditions and symmetry classes of alternating-sign matrices*, arXiv:cond-mat/0108103.